High-frequency P-wave seismic noise driven by ocean winds

Jian Zhang,[1] Peter Gerstoft,[1] and Peter M. Shearer[1]

Received 13 February 2009; revised 31 March 2009; accepted 7 April 2009; published 5 May 2009.

[1] Earth's background vibrations at frequencies below about 0.5 Hz have been attributed to ocean-wave energy coupling into the ground and propagating as surface waves and P-waves (compressional waves deep within the Earth). However, the origin and nature of seismic noise on land at frequencies around 1 Hz has not yet been well studied. Using array beamforming, we analyze the seismic noise fields at two remote sites (Parkfield and the Mojave Desert) in California, for durations of one and six months respectively. We find that (1) the seismic background noise at about 0.6–2 Hz consists of a significant amount of continuous P-waves originating offshore, and (2) the power of the P-wave noise is highly correlated with the offshore wind speed, demonstrating that these high-frequency P-waves are excited by distant ocean winds. Our result suggests a land-based seismological proxy for monitoring oceanic weather. **Citation:** Zhang, J., P. Gerstoft, and P. M. Shearer (2009), High-frequency P-wave seismic noise driven by ocean winds, *Geophys. Res. Lett.*, *36*, L09302, doi:10.1029/2009GL037761.

1. Introduction

[2] Probing the origin and propagation of Earth's background vibrations (seismic noise) has traditionally been performed for improving earthquake detection (see review by *Webb* [2002]), evaluating seismic hazard (see review by *Bonnefoy-Claudet et al.* [2006]), and more recently for imaging Earth structure [e.g., *Shapiro et al.*, 2005; *Sabra et al.*, 2005; *Courtland*, 2008]. Seismic noise from the Earth's hum (2–7 mHz) to the microseism peaks (0.05–0.5 Hz) has been associated with ocean wave activities in both theory and observations [e.g., *Longuet-Higgins*, 1950; *Webb and Cox*, 1986; *Tanimoto*, 2007a, 2007b; *Webb*, 2007; *Toksoz and Lacoss*, 1968; *Haubrich and McCamy*, 1969; *Friedrich et al.*, 1998; *Rhie and Romanowicz*, 2004; *Bromirski et al.*, 2005; *Gerstoft and Tanimoto*, 2007]. Most studies focus on surface-wave energy in seismic noise, although body waves were observed as early as the sixties [*Toksoz and Lacoss*, 1968; *Haubrich and McCamy*, 1969; *Iyer and Healy*, 1972]. Recent efforts using seismic arrays have confirmed that P-wave seismic noise correlates well with seasonal sea-state [*Koper and de Foy*, 2008; *Landès et al.*, 2008] and can even be used to track distant storms in the open ocean [*Gerstoft et al.*, 2006, 2008].

[3] Such connections between seismic observations and oceanic conditions could be made more precise through analysis of higher-frequency seismic data. It has been observed that deep ocean noise at about 0.2–16 Hz correlates with local ocean winds [*McCreery et al.*, 1993; *Wilcock et al.*, 1999; *Bromirski et al.*, 2005; *Dahm et al.*, 2006; *Vassallo et al.*, 2008]. The theory for pressure fluctuations arising from the nonlinear ocean wave interactions [*Longuet-Higgins*, 1950] has been extended to 1 Hz gravity waves by *Webb and Cox* [1986], and even to small capillary waves by *Farrell and Munk* [2008]. Depending upon the propagation efficiency of these waves, one might observe P-wave seismic noise at these high frequencies on land as well, generated from direct coupling of the deep-sea pressure fluctuations. Here we show terrestrial observations from California of continuous P-wave seismic noise at 0.6–2 Hz, which exhibit strong correlation with the ocean wind immediately offshore.

2. Data Processing and Method

[4] We analyze vertical-component seismic noise recorded at two small-aperture arrays in California (Figure 1a, Parkfield: ~11 km aperture, mid-January to mid-February in 2002; Mojave Desert Calico Fault experiment: ~4 km aperture, 6 months of data in 2006 [see *Cochran et al.*, 2009]). We apply array beamforming [*Gerstoft et al.*, 2008] to measure the noise power as a function of frequency, time, azimuth, and slowness. Based on the response to a vertically incident 1 Hz plane wave, the 3-dB beam width is 0.08 s/km for the Parkfield array and 0.12 s/km for the Calico Fault array.

[5] At Parkfield, the data were sampled at 0.025 s and split into 900-s windows. Energy of strong occasional signals (e.g., earthquakes) was reduced by truncating the amplitudes at 4 times their standard deviations, which preserves most of the noise energy. At the Calico Fault array in the Mojave Desert, the data were sampled at 0.02 s and split into 1-hour windows. Note that for the Mojave Desert data, time-domain normalization and spectral whitening are essential to reveal the P-wave noise but remove absolute amplitude. Thus, we consider only the Parkfield results when analyzing the noise power.

3. Results

[6] Slowness-azimuth spectra from 1-hour noise windows (Figure 1b) show that most 0.6–2 Hz noise energy at Parkfield comes from the coastal direction at a horizontal slowness of ~0.2 s/km, i.e., a velocity of ~5 km/s. Assuming a local/regional source, such a fast phase velocity is consistent only with P-waves that arrive from beneath the array. A similar beamformer pattern is observable at the Mojave array (Figure 1c), showing coastal noise energy arriving as P-waves. Assuming a seismic velocity versus depth model, these slownesses could be used to estimate distances to the noise source, but crustal velocity hetero-

[1]Scripps Institution of Oceanography, University of California, San Diego, La Jolla, California, USA.

0094-8276/09/2009GL037761$05.00

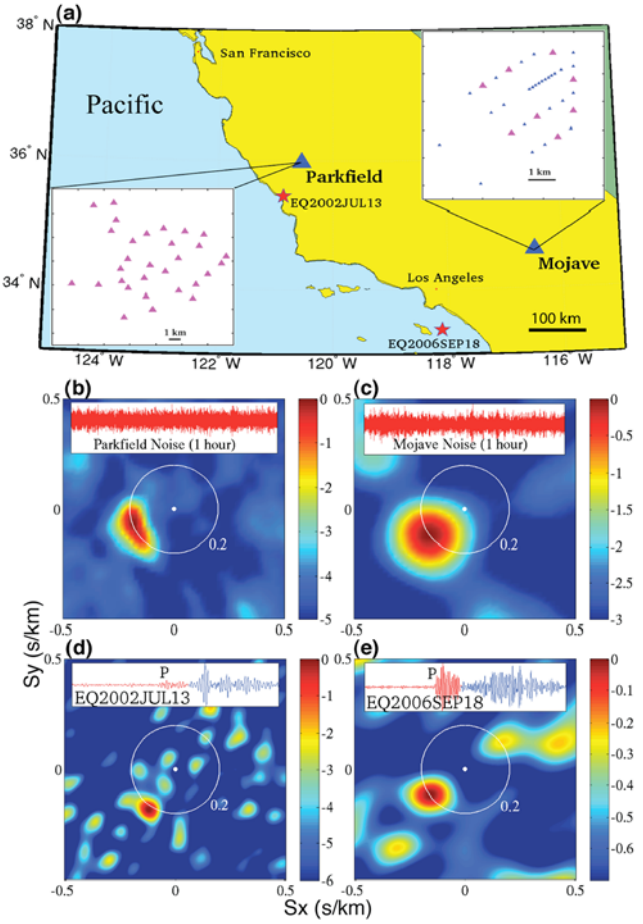

Figure 1. P-wave seismic noise and earthquakes observed from array beamforming. (a) Map of the Parkfield and Mojave arrays (triangles), as well as two earthquakes (stars) for comparison with noise observations. Slowness-azimuth spectra at 0.7–1.6 Hz are shown for (b) noise field at the Parkfield array; (c) noise field at the Mojave array; (d) P-wave part of a coastal earthquake (July 13, 2002) at the Parkfield array; and (e) P-wave part of a coastal earthquake (September 18, 2006) at the Mojave array. Example waveforms of the noise and earthquakes are shown in the inserts. The power-scale is dB.

geneities can bias these estimates. To correct for this, we calibrate the beamformer output using earthquakes with known locations in order to provide reference points for tracking the noise sources. For example, two coastal earthquakes (Figure 1a) match closely with the noise in the beamformer results. The P-wave of a coastal earthquake (July 13, 2002; M_L 1.8; 66 km SW of the Parkfield array) shows a slowness of ~0.2 s/km (Figure 1d), implying that the source of the P-wave noise observed at Parkfield is located at a similar distance from the array, i.e., offshore. A similar conclusion holds for the P-wave noise observed at the Mojave array, as the P-wave of a coastal earthquake (September 18, 2006; M_L 2.7; 203 km SW of the Mojave array) shows a slowness of ~0.18 s/km (Figure 1e).

[7] In Figure 2, we analyze the energy distribution of the P-wave noise at Parkfield derived from beamforming. From the microseism band to 2 Hz, the total noise power shows both single-frequency (SF) and double-frequency (DF) peaks, and then decreases smoothly at high frequencies (Figure 2a). The non-dispersive P-wave energy at ~0.2 s/km from ~0.6 to ~1.9 Hz is clearly revealed in the demeaned slowness-frequency spectrum (Figure 2b). Slowness-azimuth spectra in Figure 2c indicate a consistent coastal direction. The peak spreads about 45° in azimuth, indicating a wide source region. It should be noted that the high-frequency P-wave noise, although 40–60 dB weaker than the microseism energy (Figure 2a), is not accompanied by any visible surface-wave energy (slower phases). A likely explanation for this is that the P-waves are generated by deep-sea pressure fluctuations, which travel nearly vertically to the ocean bottom and thus are more efficient at generating P-waves than surface waves.

[8] This high-frequency P-wave energy is continuous in time. For example at Parkfield, despite occasional peaks due to random noise sources, the slowness of the peak spectrum (1–1.3 Hz) derived from 1-month data is consistently ~0.2 s/km (Figure 3a), while the azimuth of the energy spreads from ~225° to ~270° (Figure 3b). The peak power of the noise spectrum is shown in Figure 3c. There is no distinct diurnal/weekly variation, which is often associated with cultural noise. Furthermore, as this P-wave noise is dominant around 1 Hz, the noise power (RMS) observed from an individual Parkfield sensor reveals almost the same temporal variation of this P-wave energy (Figure 3d) as that observed from array-beamformed peaks (Figure 3c), and with a correlation-coefficient (CC) of 0.92.

[9] The beamforming results lead us to the open ocean to seek the source of the Parkfield P-wave noise. In Figure 4 we show that the high-frequency P-wave noise at Parkfield strongly correlates with the offshore winds more than 60 km (Parkfield to the coastline) away toward the southwest. Note that this differs from microseisms that have been found correlating with significant wave heights. We calculated the CC of the P-wave noise power with the wind speeds at several Pacific sites and land sites. The offshore wind data include both the *in situ* measurements at the buoys documented by the National Data Buoy Center (NDBC), and the hindcast wind fields for the Wave Information Studies (WIS) program conducted by the Coastal and Hydraulics Laboratory. The data for land sites are available from the National Climatic Data Center.

[10] It can be seen in Figure 4a that, in general, Pacific sites SW of Parkfield all show high correlations, in agreement with the direction of the noise observed from beamforming (225–270°). In contrast, the correlation is poor at all land sites. Although both the speed and direction of the wind are probably relatively homogeneous over a broad region of ocean, Figure 4a shows that the highest correlation (CC = 0.88) is obtained at a site with azimuth 248° (WIS 192), suggesting that the offshore winds with the shortest distance to Parkfield may contribute most to the P-wave noise at Parkfield. We also found that each WIS hindcast wind provides higher correlation than its nearby buoy wind. A reasonable explanation is that the hindcast winds, as developed by considering all available wind measurements and interpolated to a 1-degree spatial grid (J. L. Hanson and R. E. Jensen, Wave system diagnostics for numerical wave models, paper presented at the 8th International Workshop on Wave Hindcasting and Forecasting, Environment Canada,

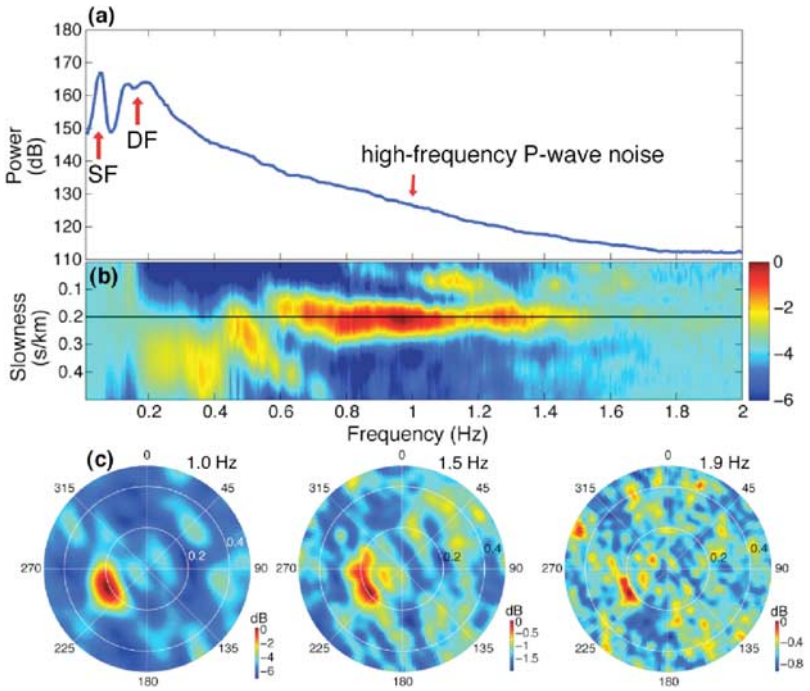

Figure 2. One-day (Julian Day 15, 2002) Parkfield noise spectra derived from beamforming. (a) Power spectrum. SF, single-frequency microseism peak; DF, double-frequency microseism peak; (b) slowness-frequency spectrum (dB) demeaned at each frequency, which emphasizes energy phases rather than absolute power; (c) slowness-azimuth spectra (in relative dB) for the frequencies around 1.0, 1.5, and 1.9 Hz respectively.

Oahu, Hawaii, 2004), represent a broad-surface average at each point and thus correlate better with the P-wave noise that is likely generated over a large sea area.

[11] Example time series of the wind speeds, wind directions, and significant wave heights are shown in Figure 4b for the WIS 192 and its nearby buoy 46028. The wind direction is relatively stable (from NW) over time. The significant wave height shows clear differences from the wind speed, as it is dominated by swells that originate from distant storms. Besides the high CC values, the strong correlation of the P-wave noise power at 1 and 1.5 Hz with the wind speed at the WIS 192 is evidenced by a comparison of their time series in Figures 4c and 4d respectively, demonstrating that the high-frequency P-wave seismic noise at Parkfield is generated by the ocean winds off the coast. The scatter plots of power in dB as a function of wind speed are also shown, suggesting that the increase in noise power with wind speed is roughly 1 dB per m/s.

4. Discussion and Conclusions

[12] It is likely that the wind energy couples into the P-wave noise via wind-generated ocean waves. At 1–2 Hz, the ocean waves have wavelengths of about 1.5–6 m and are generated by local ocean winds, in contrast to the much longer wavelengths (~150 m) and stronger swells generated by distant storms. In Figures 4c–4d, an empirical power-law form $\log P = c + b \cdot V^a$ (P is noise power and V is wind speed) fits the data well for "a" close to but likely less than 1. This may reflect saturation of noise power for higher wind speed, though less strong than for *McCreery et al.* [1993]. It is also noteworthy that the correlation lag-time of the full-length time series is about 3 hours, which may

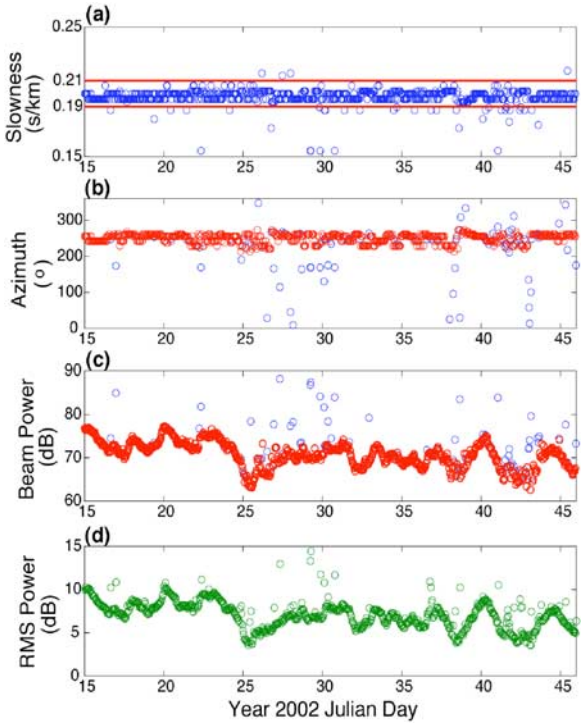

Figure 3. Temporal variations of the Parkfield noise at 1.0–1.3 Hz. (a) Slowness, (b) azimuth, and (c) power of the peak energy from beamforming. In Figures 3b and 3c, points corresponding to the slowness within 0.19–0.21 s/km (lines in Figure 3a) are in red. (d) RMS power of the noise recorded at a single station of the Parkfield array. The dB scale for Figures 3c and 3d is arbitrary.

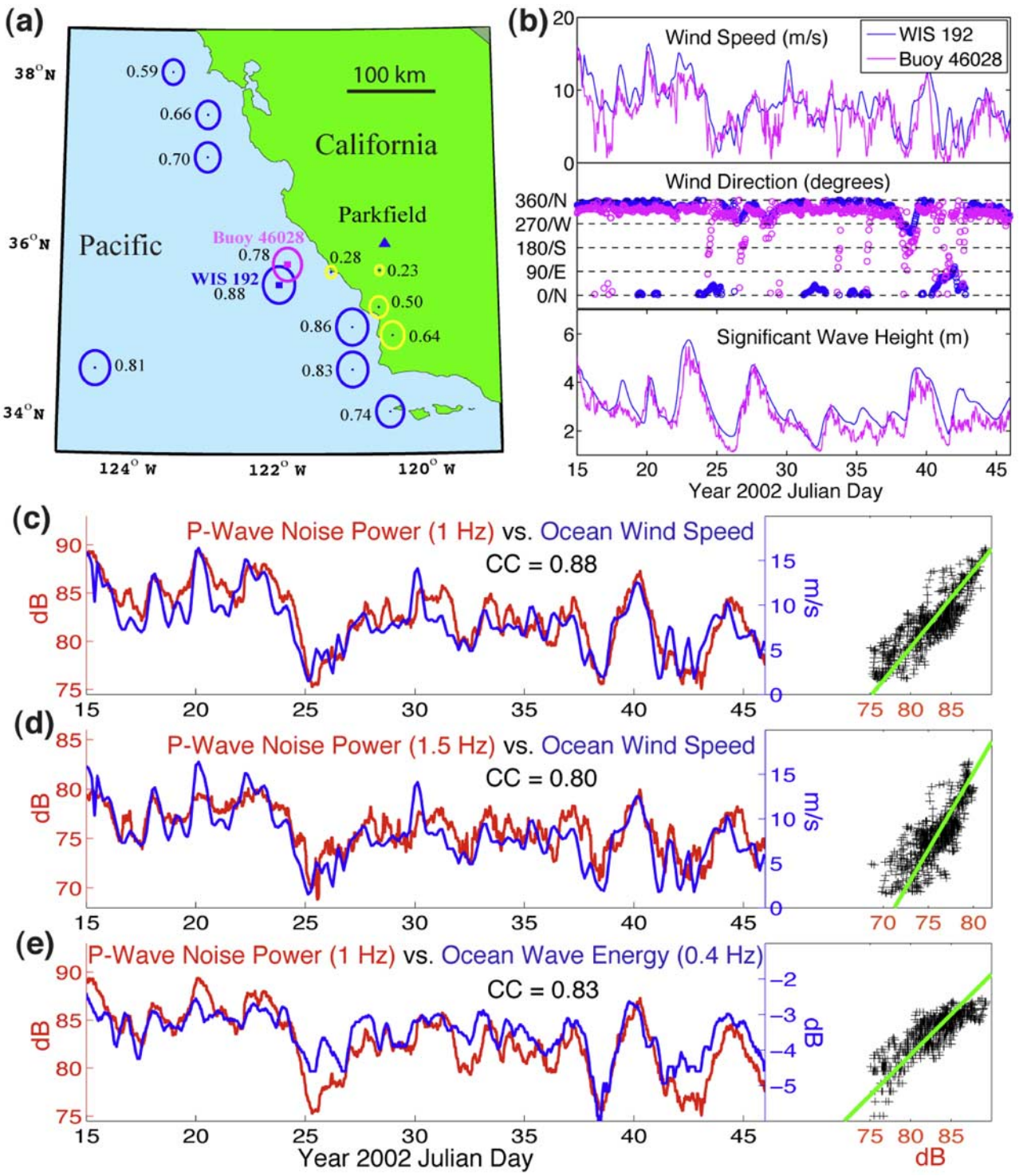

Figure 4. Correlation of the Parkfield P-wave noise power with the wind speeds at some offshore and onshore sites. (a) Map of the Parkfield array (triangle) and some wind stations (circles with blue for 8 WIS stations, pink for a NDBC buoy, and yellow for 4 land sites). The circle size indicates the correlation-coefficient (CC) at 1 Hz for each station as marked. (b) The wind speeds, wind directions, and significant wave heights at the WIS 192 and at its nearby NDBC buoy 46028. (c) Time series of 1 Hz noise power versus wind speed at the WIS 192. (d) 1.5 Hz noise power versus wind speed at the WIS 192. (e) 1 Hz noise power versus 0.4 Hz wave energy (dB, relative to 1 m^2/Hz) at the buoy 46028.

reflect the response time of the wind-generated waves. However, the lag-time appears uneven and seems to be longer when the wind is decreasing rapidly (e.g., Julian Day 24 and 37), which agrees with the wind-wave behavior suggested by *Young* [1999], i.e., a slower response of the ocean-wave spectrum to a decrease than to an increase in wind speed.

[13] The simplest generation mechanism is the direct coupling of the vertical pressure fluctuations due to nonlinear wave-wave interaction [*Longuet-Higgins*, 1950]. Such pressure fluctuations peak at twice the ocean wave frequency. As the P-wave energy peaks near 1 Hz, in Figure 4e we compare the P-wave noise power at Parkfield with the ocean wave energy at 0.4 Hz (upper limit of spectral wave density data from buoy 46028, which corresponds to 0.8 Hz seismic frequency) and find a strong correlation as well (CC = 0.83). This agrees with the Longuet-Higgins hypothesis. However given the uniform wind direction (Figure 4b), it is not yet clear if the open-ocean wind waves propagate at sufficiently different directions to create wave-wave interaction.

[14] As wind blows over broad regions, P-waves should be also generated in the ocean outside of the observed azimuth range (225–270°). However, these P-waves would attenuate more due to their longer propagation distance to the array, and thus generally appear weaker in the beam-former output. Although observed at the Mojave array as well (~200 km to the coast), how far inland this type of energy can be detected will depend upon the strength of the originating winds, the attenuation of the P-waves with distance, and the amplitude of other possible noise sources.

[15] The strong correlation between the P-wave noise and the ocean wind speed potentially allows seismic stations on land to be used for measuring offshore winds, of which the daily fluctuations are reasonably well captured (Figures 4c and 4d). These observations suggest it should be possible to further study the mechanism of how wind-generated ripples can reach the sea floor by using a seismic array designed to image energy for higher frequencies, without the need of ocean-bottom deployments [*Elgar*, 2008]. Moreover, recent advances in imaging Earth's structure using cross-correlation of seismic noise have focused on surface waves, while efforts to extracting Earth's response from body-wave noise are still rare. The observations of P-wave seismic noise from this work and elsewhere suggest that analysis of body-wave noise may provide new avenues for probing Earth's structure.

[16] **Acknowledgments.** We thank Elizabeth Cochran and the field crew responsible for the 2006 Calico Experiment in the Mojave. We are grateful to Barbara Tracy and Alan Cialone, U.S. Army Coastal and Hydraulics Laboratory, for their wind data. The facilities of the IRIS Data Management System were used for access to the seismic data. This work was supported by U.S. Air Force Research Laboratory, FA8718-07-C-0005.

References

Bonnefoy-Claudet, S., F. Cotton, and P. Bard (2006), The nature of noise wavefield and its applications for site effects studies—A literature review, *Earth Sci. Rev.*, *79*, 205–227.

Bromirski, P. D., F. K. Duennebier, and R. A. Stephen (2005), Mid-ocean microseisms, *Geochem. Geophys. Geosyst.*, *6*, Q04009, doi:10.1029/2004GC000768.

Cochran, E. S., Y.-G. Li, P. M. Shearer, S. Barbot, Y. Fialko, and J. E. Vidale (2009), Seismic and geodetic evidence for extensive, long-lived fault damage zones, *Geology*, *37*, 315–318.

Courtland, R. (2008), Harnessing the hum, *Nature*, *453*, 146–148.

Dahm, T., F. Tilmann, and J. P. Morgan (2006), Seismic broadband ocean-bottom data and noise observed with free-fall stations: Experiences from long-term deployments in the North Atlantic and the Tyrrhenian Sea, *Bull. Seismol. Soc. Am.*, *96*, 647–664.

Elgar, S. (2008), Ripples run deep, *Nature*, *455*, 888.

Farrell, W. E., and W. Munk (2008), What do deep sea pressure fluctuations tell about short surface waves?, *Geophys. Res. Lett.*, *35*, L19605, doi:10.1029/2008GL035008.

Friedrich, A., F. Kruger, and K. Klinge (1998), Ocean-generated microseismic noise located with the Grafenberg array, *J. Seismol.*, *2*, 47–64.

Gerstoft, P., and T. Tanimoto (2007), A year of microseisms in southern California, *Geophys. Res. Lett.*, *34*, L20304, doi:10.1029/2007GL031091.

Gerstoft, P., M. C. Fehler, and K. G. Sabra (2006), When Katrina hit California, *Geophys. Res. Lett.*, *33*, L17308, doi:10.1029/2006GL027270.

Gerstoft, P., P. M. Shearer, N. Harmon, and J. Zhang (2008), Global P, PP, and PKP wave microseisms observed from distant storms, *Geophys. Res. Lett.*, *35*, L23306, doi:10.1029/2008GL036111.

Haubrich, R. A., and K. McCamy (1969), Microseisms: Costal and pelagic sources, *Rev. Geophys.*, *7*, 539–571.

Iyer, H. M., and J. H. Healy (1972), Evidence for the existence of locally-generated body waves in the short-period noise at the Large Aperture Seismic Array, Montana, *Bull. Seismol. Soc. Am.*, *62*, 13–29.

Koper, K., and B. de Foy (2008), Seasonal anisotropy of short-period seismic noise recorded in south Asia, *Bull. Seismol. Soc. Am.*, *98*, 3033–3045.

Landès, M., F. Hubans, N. M. Shapiro, A. Paul, and M. Campillo (2008), Studying the origin of deep ocean microseisms using teleseismic body waves, *Eos Trans. AGU*, *89*(53), Fall Meet. Suppl., Abstract S31A-1893.

Longuet-Higgins, M. S. (1950), A theory of origin of microseisms, *Philos. Trans. R. Soc. London, Ser. A.*, *243*, 1–35.

McCreery, C. S., F. K. Duennebier, and G. H. Sutton (1993), Correlation of deep ocean noise (0.4–30 Hz) with wind, and the Holu spectrum—A worldwide constant, *J. Acoust. Soc. Am.*, *93*, 2639–2648.

Rhie, J., and B. Romanowicz (2004), Excitation of Earth's continuous free oscillations by atmosphere-ocean-seafloor, *Nature*, *431*, 552–556.

Sabra, K. G., P. Gerstoft, P. Roux, W. A. Kuperman, and M. C. Fehler (2005), Extracting time-domain Green's function estimates from ambient seismic noise, *Geophys. Res. Lett.*, *32*, L03310, doi:10.1029/2004GL021862.

Shapiro, N. M., M. Campillo, L. Stehly, and M. H. Ritzwoller (2005), High-resolution surface wave tomography from ambient seismic noise, *Science*, *307*, 1615–1617.

Tanimoto, T. (2007a), Excitation of microseisms, *Geophys. Res. Lett.*, *34*, L05308, doi:10.1029/2006GL029046.

Tanimoto, T. (2007b), Excitation of normal modes by nonlinear interaction of ocean waves, *Geophys. J. Int.*, *168*, 571–582.

Toksoz, M. N., and R. T. Lacoss (1968), Microseisms: Mode structure and sources, *Science*, *159*, 872–873.

Vassallo, M., A. Bobbio, and G. Iannaccone (2008), A comparison of sea-floor and on-land seismic ambient noise in the Campi Flegrei Caldera, southern Italy, *Bull. Seismol. Soc. Am.*, *98*, 2962–2974.

Webb, S. C. (2002), Seismic noise on land and on the sea floor, in *International Handbook of Earthquake and Engineering Seismology*, *Int. Geophys. Ser.*, vol. 81, edited by W. H. K. Lee, pp. 305–318, Academic, Amsterdam.

Webb, S. C. (2007), The Earth's 'hum' is driven by ocean waves over the continental shelves, *Nature*, *445*, 754–756.

Webb, S. C., and C. S. Cox (1986), Observations and modeling of seafloor microseisms, *J. Geophys. Res.*, *91*, 7343–7358.

Wilcock, W. S. D., S. C. Webb, and I. T. Bjarnason (1999), The effect of local wind on seismic noise near 1 Hz at the MELT site and in Iceland, *Bull. Seismol. Soc. Am.*, *89*, 1543–1557.

Young, I. R. (1999), *Wind Generated Ocean Waves*, *Elsevier Ocean Eng. Book Ser.*, vol. 2, Elsevier, New York.

P. Gerstoft, P. M. Shearer, and J. Zhang, Scripps Institution of Oceanography, University of California, San Diego, La Jolla, CA 92093-0238, USA. (jianz@ucsd.edu)